Available online at www.sciencedirect.com
ScienceDirect
International Journal of Thermal Sciences 47 (2008) 147–156
International Journal of Thermal Sciences
www.elsevier.com/locate/ijts

Determination of atherosclerotic plaque temperature in large arteries

O. Ley *, T. Kim

Texas A&M University, Department of Mechanical Engineering, College Station, TX 77843-3123, USA

Received 28 September 2006; received in revised form 15 January 2007; accepted 24 January 2007

Available online 3 April 2007

Abstract

Atherosclerotic plaques with high probability of rupture can be characterized by the presence of a hot spot in the arterial wall, which forms due to accumulation of inflammatory cells in the plaque. This paper presents calculations of the arterial wall temperature distribution of arteries affected by plaque. This analysis characterizes the factors affecting plaque temperature, such as vessel geometry, plaque size, inflammatory cell density and distribution, and blood flow pattern. Three vessel types which present high occurrence of plaque are studied: a stenotic straight artery, an arterial bend and an arterial bifurcation corresponding to a human aorta, a coronary artery and a carotid bifurcation, respectively. The atherosclerotic plaque is located in the sites of low shear stress, and a local heat generation is introduced to account for the presence of inflamed plaque.

It is shown that the plaque temperature correlates positively to inflammatory cell density and layer thickness, whereas the plaque temperature varies inversely with the depth of the inflammatory cell layer or fibrous cap. From the calculations, it is observed that the best spot to measure plaque temperature is between the middle and the far edge of the plaque where maximum temperature is located. The results contribute to understanding the physical characteristics of the plaque structure and its relationships to plaque temperature, and also suggest a tool to understand the arterial wall temperature measurements obtained with novel catheters.

PACS: 44.05.+e; 44.15.+a; 47.55.pb; 47.63.Cb; 81.70.Pg

Keywords: Atherosclerotic plaque; Inflammatory cell; Blood flow; Arterial wall temperature; Inflammatory process; Metabolic heat; Flow instabilities; Blood vessel

1. Introduction

Atherosclerosis is characterized by the accumulation of fatty deposits (lipid) and connective tissue on the arterial wall [1]. These deposits, known as plaque, can eventually obstruct blood flow, predispose the vessel to thrombosis and impair the elastic response of the vessel to hydrodynamic stress [2]. According to recent studies, vulnerable plaque, or plaque with high likelihood of rupture, are linked with the appearance of hot spots on the arterial wall [3], such temperature increments are caused by the presence of macrophages or inflammatory cells embedded in the plaque [4].

Based on the temperature heterogeneity produced by plaque inflammation, and the fact that plaque composition rather than degree of stenosis determines the likelihood of rupture [5–7], there is a marked interest in monitoring and understanding arterial wall temperature and the physical and physiological factors that affect the temperature. Several techniques to measure arterial wall temperature have been recently developed for clinical practice with the objective of detecting vulnerable atherosclerotic plaques that might lead to cardiovascular complications followed by plaque rupture [8]. Thermal analysis and monitoring of atherosclerotic plaques can help on early detection and follow up in specific patient population. The current technique involves the use of novel basket catheters containing an array of temperature sensors, which are used to measure the temperature around the interior circumference of the artery at a given location [9].

* Corresponding author.
E-mail addresses: oley@tamu.edu (O. Ley), taehong-kim@tamu.edu (T. Kim).

1290-0729/$ – see front matter
doi:10.1016/j.ijthermalsci.2007.01.034

Nomenclature

C_p	Specific heat	$J\,kg^{-1}\,°C^{-1}$
d_{mp}	Macrophage layer thickness	μm
d_p	Plaque thickness ($d_p = \alpha d_w$), where $\alpha = 1, 2, 3$	μm
d_w	Arterial wall thickness	μm
k	Thermal conductivity	$W\,m^{-1}\,°C^{-1}$
L	Arterial length along the vessel axis	mm
l_f	Fibrous cap thickness	μm
l_{mp}	Macrophage layer length ($l_{mp} = \beta l_p$), where $\beta = 0.5, 0.25$	μm
l_p	Plaque length	mm
ℓ	Position along the vessel axis	
P	Pressure	$N\,m^{-2}$
q_{cell}	Heat produced by a single cell	W
$\dot{q}_m$	Tissue metabolic heat	$W\,mm^{-3}$
R	Vessel radius	mm
R_o	Vessel radius at the inlet $\ell = 0$	mm
Re	Reynolds number	
Re_{max}	Maximum Reynolds number	
Re_{mean}	Mean-reference Reynolds number	
T	Temperature	°C
T_a	Arterial temperature	°C
T_{max}	Maximum temperature	°C
u_o	Blood velocity at the inlet ($\ell = 0$)	$m\,s^{-1}$
V_{cell}	Volume of a single cell	mm^3
$\mathbf{v}$	Blood velocity vector and components (u, v, w)	$m\,s^{-1}$
WSS	Wall shear stress	$N\,m^{-2}$
ΔA	Each element area	m^2
A_{tot}	Total wetted area	m^2

Greek symbols

α_w	Womersley number	
γ	Thermal diffusivity	$m^2\,s^{-1}$
ρ	Density	$kg\,m^{-3}$
μ	Viscosity	Pa s
ξ	Vorticity	s^{-1}
Γ_{ABS}	Modified or absolute circulation	$m^2\,s^{-1}$

Subscripts

ABS	Absolute value
f	Fibrous cap
m	Metabolic activation
mp	Macrophage layer
p	Plaque
tot	Total value
w	Arterial wall

In vivo arterial wall temperature measurement has limitations caused by cooling effect of blood flow, improper contact between arterial wall and temperature sensor, possibility of plaque disruption while measuring the sensitive plaque surface with the novel catheters, and occlusion of blood flow in vessel, which introduce the need to create mathematical models to investigate the relations among plaque temperature, blood flow, plaque geometry and composition. Recently, a numerical study of temperature distribution in the coronary artery was presented with a simplified model [10]. However, anatomically correct plaques were not considered to observe the combined effect of the convective cooling associated to the blood flow and the metabolic production in the macrophage layer.

According to clinical and postmortem anatomical studies, atherosclerotic lesions in humans develop preferentially at the inner walls of curved segments in relatively large arteries but the outer walls in case of bifurcations [4,11] regardless of diet and ethnicity [4]. The vulnerable sites are correlated to locations where the fluid shear stress on the vessel wall is significantly lower in magnitude than the normal physiological value [12–14]. The blood flow in such sites is disturbed by the occurrence of flow separation and the formation of complex secondary and circulation flows [15,16].

In this paper, the plaque is located in the region of minimal shear stress identified after solving the Navier–Stokes equations in the arteries selected. The arterial wall temperature distribution is calculated solving the energy equation which incorporates the heat generation produced by the macrophage cells in the plaque. For the calculations, three different types of arteries are considered, which are known to commonly develop atherosclerotic plaques. Detailed plaque structure based on anatomical descriptions of atherosclerotic deposits is considered to describe the plaque containing the macrophage cells [17].

This model is used to determine the plaque temperature distribution and the effect of vessel geometry, blood flow, inflammatory cell density, and plaque size and composition. The calculations presented aim to better understand the temperature profiles measured with novel catheters and reveal information about the temperature maps of atherosclerotic plaques during inflammatory process.

2. Mathematical model

2.1. System description

The blood vessel shapes considered are: a stenotic straight artery, a bending artery and an arterial bifurcation corresponding to the geometry and dimensions of a human aorta, a coronary artery and a carotid bifurcation, respectively, illustrated in Fig. 1 and Table 1. The geometry of the straight artery is obtained from a medium-sized human artery of Stangeby and Ethier's study [18]. The shape of the bending artery is modified from an anatomical realistic arterial model of Wada and Karino's study [16] based on a photograph of the human coronary artery used in the flow study of Asakura and Karino [19]. The geometry of arterial bifurcation is taken from the studies of a human carotid artery by Perktold et al. [20] and Filipovic and

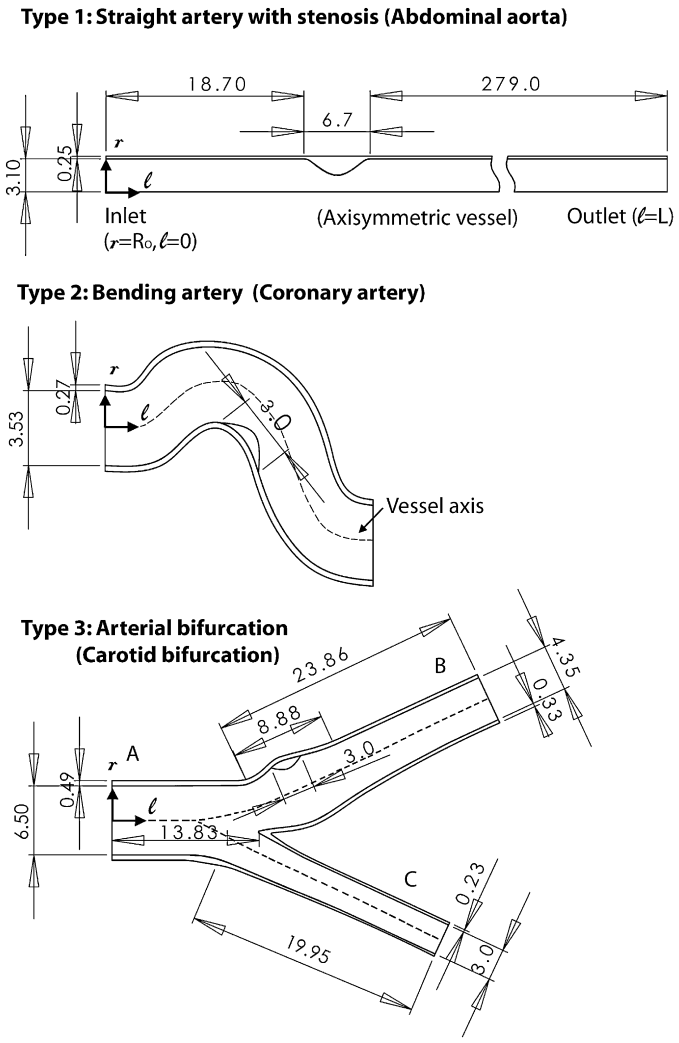

Fig. 1. Vessel types considered in this paper and the corresponding geometrical parameters used to describe the vessels. The dimension presented are shown in millimeters.

Table 1
Geometric parameters of the different vessel types used in this study

Vessel type	Radius R (mm)	Length L (mm)	Thickness d_w (mm)
Type 1	3.10	304.4	0.25
Type 2	1.765	17.2	0.27
Type 3			
Segment A	3.25	13.83	0.49
Segment B	2.175	23.86	0.33
Segment C	1.5	19.95	0.23

L is the distance along the axis of the vessel which is always perpendicular to the radius.

Kojic [21]. In each one of these vessels, the blood velocity distribution is calculated to determine the region prone to develop atherosclerosis, and the temperature distribution is investigated in the plaque region for different plaque sizes and various concentrations of macrophages or inflammatory cells.

This work studies the effect of plaque structure and composition over the location of the hot spots and the maximum temperature registered for a given inflammatory cell density

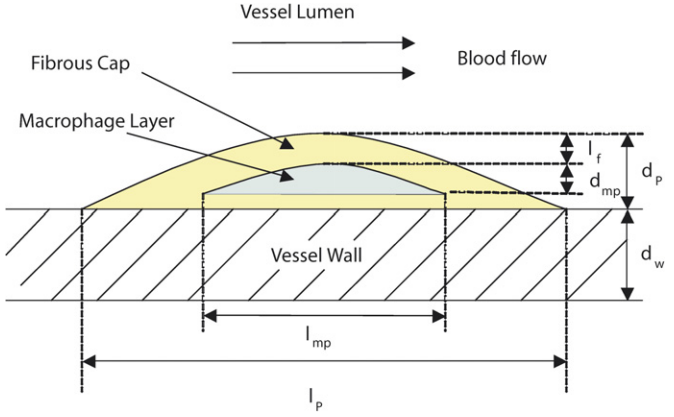

Fig. 2. Plaque geometry and dimensions. d_w is the arterial wall thickness, d_p is the plaque thickness, d_{mp} is the macrophage rich layer thickness, l_f is the thickness of the fibrous cap. l_p and l_{mp} represent the extension or length of the plaque and the macrophage layer in the longitudinal direction, respectively.

and distribution. In this paper, steady state calculations are performed, such calculations have been justified by the observations in literature [22,23]; the oscillatory nature of the flow ($Re_{mean} = 300$, Womersley number $\alpha_w = 4$) does not affect significantly the transport and deposit of macromolecules on the vessel wall compared to steady state calculations of $Re = 448$. By convention, Womersley number of the pulsatile flow ranges from 1 to 10 for medium-sized vessels such as coronary and carotid arteries [24,25].

2.2. Plaque composition, size and distribution

Hot spots in the atherosclerotic plaque are formed as the macrophages in the lesions become active, which occurs when an inflammatory process develops. The macrophages or inflammatory cells are embedded in the plaque forming a thin layer [17]. The lesion starts by adhesion and filtration of monocytes (Mo) and low density lipoproteins (LDL) over the endothelium. This process occurs at regions of low shear stress. After filtration, the monocytes are transformed into macrophages (Mc) and engulf LDL molecules to form foam cells (FC), this process gradually increases the size of the plaque and makes the plaque evolve depending on the components that filtrate and deposit. A detailed description of the evolution, composition and classification of atherosclerotic plaque can be found in [17,26].

The temperature change in the vulnerable plaque is correlated to the macrophage density and distribution, as well as the depth from the lumen surface at which the layer of macrophages are located. Vulnerable plaques showing thermal inhomogeneities of 0.4 to 2.2 °C have a thickness of 400 μm and a macrophage rich layer of between 15 to 40 μm thick [27]. In this study, the plaque size and the macrophage rich layer are defined by variable parameters as described in Fig. 2, where a longitudinal section of an atherosclerotic blood vessel containing a layer of macrophages is shown.

In Fig. 2, the arterial wall thickness (d_w) is set to be 5 to 10% the vessel diameter (d_o), which has been reported for human arteries in the literature [16,18,28,29]. The plaque is located over the arterial wall, and its thickness (d_p) is chosen to be $d_p = \alpha d_w$,

where $\alpha = 1, 2$; these values of α represent the case of plaques that produce small occlusions, which are difficult to observe with MRI or other contrast agent methods [30]. l_f is the distance between the vessel lumen and the macrophage layer, and physically represents the thickness of the fibrous cap; for the calculations l_f is set to 50 and 100 μm; these values will be served to analyze the effect on the plaque temperature gradient when the heat source is at different depths. Finally, l_p and l_{mp} denote the extension of the plaque and macrophage layer in the longitudinal direction of the vessel, respectively. The plaque is located in the regions that correspond to the lowest wall shear stress, and l_p is extended to cover these regions in each one of the vessel types considered. The dimension l_{mp} is given by $l_{mp} = \beta l_p$, where $\beta = 0.5$ and 0.25; these values of β were selected from experiments showing high macrophage concentration at the center of the lesion [17].

2.3. Blood flow calculations

In this study, two-dimensional steady-state blood flow is governed by the continuity equation and Navier–Stokes equations for a homogeneous and incompressible fluid:

$$\nabla \cdot \mathbf{v} = 0 \tag{1}$$

$$\rho(\mathbf{v} \cdot \nabla)\mathbf{v} = -\nabla P + \mu \nabla^2 \mathbf{v} \tag{2}$$

where $\mathbf{v}$ is the velocity vector of the blood, P the blood pressure, ρ the density and μ the viscosity of the blood. Cartesian coordinate system (r, ℓ) is positioned at the center of the vessel entrance ($\ell = 0$ and $r = 0$). R_o and L are the radius and the outlet of each vessel, respectively, in Fig. 1.

For boundary conditions, no-slip conditions are imposed on the velocities at the arterial walls, $u = 0$ and $v = 0$ at $r = R_o$. At the outlet of the artery $\ell = L$, the gauge pressure is set to zero for a fully developed flow, $P = 0$. Especially, axi-symmetric condition is used at the centerline of straight artery, $\frac{\partial u}{\partial r} = 0$ at $\ell = L$. At the inlet ($\ell = 0$), a fully developed velocity profile is assumed as

$$u = 2u_o\left(1 - \left(\frac{r}{R_o}\right)^2\right), \quad v = 0 \quad \text{at } \ell = 0 \tag{3}$$

where u and v represent the longitudinal and radial velocity at the inlet. u_o is the mean velocity at the inlet. Reynolds numbers of 300 and 500 are applied to represent the mean-reference and maximum velocities, respectively, during a cardiac cycle based on the following literature:

(1) for calculations of straight artery, pulsatile functions with $Re_{mean} = 200$ and 300 were used for mean velocities in [24, 31].
(2) A transient simulation in human coronary arteries is performed under physiological function with $Re_{mean} = 200$ and $Re_{max} = 410$ [32].
(3) In experimental study of carotid bifurcation, Reynolds numbers of peak flow velocities were $Re = 160$ and 560 [33].

2.4. Temperature prediction at the arterial wall

Given the fact that plaque vulnerability is related to temperature inhomogeneities within the arterial wall of an atherosclerotic artery, the temperature field in a blood vessel is calculated by solving the energy equation. The arteries are modeled as a vessel which contains a region capable of producing heat (macrophage layer). Heat convection due to blood flow in the arterial lumen and heat conduction through the vessel walls are considered. The steady state energy equation takes the form

$$\rho_i C_{pi}(\mathbf{v} \cdot \nabla) T_i - \nabla \cdot (k_i \nabla T_i) = \dot{q}_{mi} \tag{4}$$

where i refers to the different regions present in the system, that correspond to blood, arterial wall, plaque and macrophage layer. T_i represents the temperature, $\mathbf{v}$ is the velocity of blood in the lumen region, k_i the thermal conductivity, ρ_i the density, and C_{pi} the specific heat. $\dot{q}_{mi}$ represents the metabolic heat produced by the inflamed plaque. It is assumed that the heat generation in the arterial wall is negligible, and the only region with considerable heat generation is the macrophage layer. The values of the thermal parameters for the blood, arterial wall and plaque can be found in the literature [34–36] and are shown in Table 2.

The metabolic heat released by the inflamed plaque is a direct function of the plaque composition and the developmental stage of the lesion. Macrophages are involved in all evolutionary stages of the lesion, but their activation and subsequent metabolic heat production varies in each stage. Virmani et al. reported that the atherosclerosis before plaque rupture experiences three stages [17]. To account for the heat produced by macrophages at the different activation stages, three different values for the heat generation of the macrophage layer corresponding to $\dot{q}_m = 0.05, 0.1$ and $0.2\ \mathrm{W\,mm^{-3}}$ are used. The values of $\dot{q}_m$ for the macrophage layer are approximated from the following expression

$$\dot{q}_m \left[\frac{\mathrm{W}}{\mathrm{mm}^3}\right] = \frac{q_{cell}}{V_{cell}} \tag{5}$$

where q_{cell} is the heat produced by a single cell and V_{cell} is the volume of a single cell. It is reported that the metabolic heat of q_{cell} is dependent on the kind and concentration of macrophage cells; in the case of rabbit, alveolar macrophage produces around 20 pW per cell and other cells with high metabolic activity, such as hepatocytes, produce 300 pW per cell [37]. In this study, q_{cell} is assigned to produce a maximum temperature change comparable with the reported measurement [3,38].

Table 2
Thermophysical parameters of blood, arterial wall, plaque tissue and macrophage layer

	Blood	Arterial wall	Plaque	Macrophage layer
k_i ($\mathrm{W\,m^{-1}\,°C^{-1}}$)	0.549	0.476	0.484	0.484
ρ_i ($\mathrm{kg\,m^{-3}}$)	1050	1075	920	920
C_{pi} ($\mathrm{J\,kg^{-1}\,°C^{-1}}$)	4390	3490	4080	4080
μ_i (Pa s)	0.0033			

These parameters where taken from [35].

The following boundary conditions are considered for the energy equation (4), which correspond to: constant temperature at the external vessel wall justified by the fact that vessel wall is well perfused by the vasa vasorum

$$T = T_a \quad \text{at } r = R \tag{6}$$

constant blood and tissue temperature at the entrance of the vessel

$$T = T_a \quad \text{at } \ell = 0 \tag{7}$$

and no temperature gradient at the vessel outlet

$$\frac{\partial T}{\partial n} = 0 \quad \text{at } \ell = L \tag{8}$$

where T_a is a constant that represents the arterial or core temperature and was assigned a value of 37.5 °C. Eq. (8) represents how blood flow removes heat from the vessel wall by convection. Finally, continuity of heat flux and temperature at the lumen–plaque interface, the plaque–vessel wall interface and the plaque–macrophage layer interface are assumed.

2.5. Solution procedure

Unstructured mesh consisting of triangular elements is generated for the geometry. The mesh distribution was refined around the plaque and macrophage layer regions because large temperature and velocity gradients were expected in the region surrounding the plaque and heat source. The average numbers of triangular elements used in the calculation are 34 000 for straight artery, 28 000 for bending artery, and 25 000 for bifurcation artery, depending on the artery geometry and the structure of plaque and macrophage layer.

In this study, commercially available multi-physics software package COMSOL Multiphysics in version 3.2 (COMSOL, Inc.) for the finite element method is used for modelling and solving coupled physics problems of the blood flow and the heat transfer fields with heat generation in a two-dimensional steady-state problem. Convergence was obtained when the relative tolerances to control the error in each integration step was less than 1×10^{-6} for the temperature and the velocity solutions, which the number of iteration was 25 for all the arterial cases. Grid independence was verified by varying the mesh density under each arterial model at $Re = 300$. The finer meshes were performed, which had 70 000, 50 000 and 50 000 elements for straight artery, bending artery and arterial bifurcation, respectively.

3. Results

In this study, the temperature inhomogeneity is characterized with the following parameters:

(1) the arterial geometry and plaque location (Fig. 1),
(2) the heat generation produced by the macrophage layer ($\dot{q}_m$),
(3) the thickness and length of the macrophage layer (d_{mp} and l_{mp}),
(4) the depth at which the macrophage layer is encountered (l_f), and
(5) the thickness of the atherosclerotic plaque ($d_p = \alpha d_w$).

For the calculations, the parameters shown in Table 2 are used; to check the sensibility of unknown parameters, such as the plaque thermal conductivity, the value of k for the plaque and macrophage layer was varied ±20%. Variations of the maximum temperature registered in the plaque lumen interface was of 0.01 °C. The plots presented herein indicate the temperature change $\Delta T = (T - T_a)$ along the plaque surface for each one of the arterial geometries considered. A coordinate system is defined such that the horizontal axis coincides with the base of the plaque. In order to compare with the different arteries studied, the horizontal position is divided by the plaque length (l_p).

3.1. Variation of q_m

Figs. 3, 4 and 5 indicate how the temperature at the plaque/lumen interface changes when the metabolic heat in the macrophage layer takes the values of $\dot{q}_m = 0.05$, 0.1 and 0.2 W mm^{-3}. The temperature distribution in the three vessels presents a maximum, which value is proportional to $\dot{q}_m$, and its magnitude varies with the arterial geometry. The largest increase of temperature change ΔT is observed $0.03 < \Delta T < 1.6$ at the arterial bifurcation, and the smallest increase occurs $0 < \Delta T < 0.8$ at the bending artery. It is observed that the arterial geometry affects the temperature distribution, as well as the location of the maximum temperature change $\Delta T_{max} = (T_{max} - T_a)$ over the plaque/lumen interface. In the bending artery, ΔT_{max} occurs closer to the center of the macrophage layer; where as, in the straight artery and arterial bifurcation,

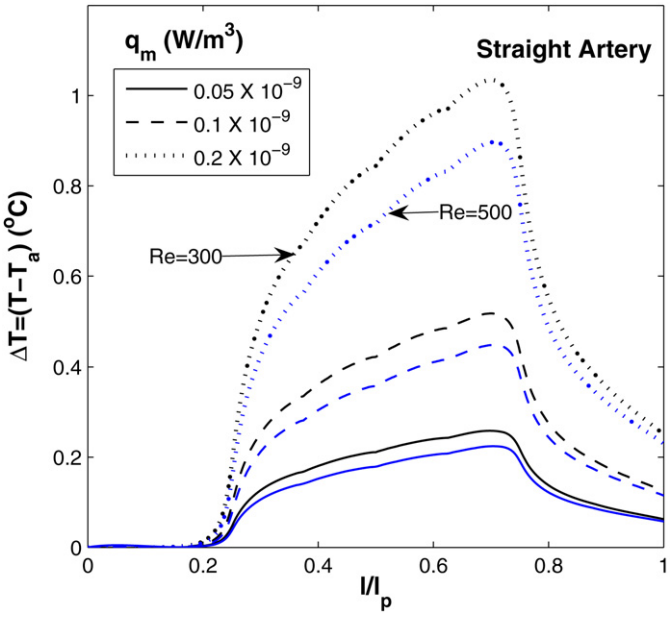

Fig. 3. Temperature change at the plaque/lumen interface produced by variations in the local heat generation in the plaque $\dot{q}_m$ for a straight artery with stenosis. In this figure, the macrophage layer dimensions are $l_{mp} = 3.335$ μm ($l_{mp} = l_p/2$) and $d_{mp} = 25$ μm, $d_p = 250$ μm, and $l_f = 50$ μm. The black lines correspond to $Re = 300$ and the gray lines represent $Re = 500$.

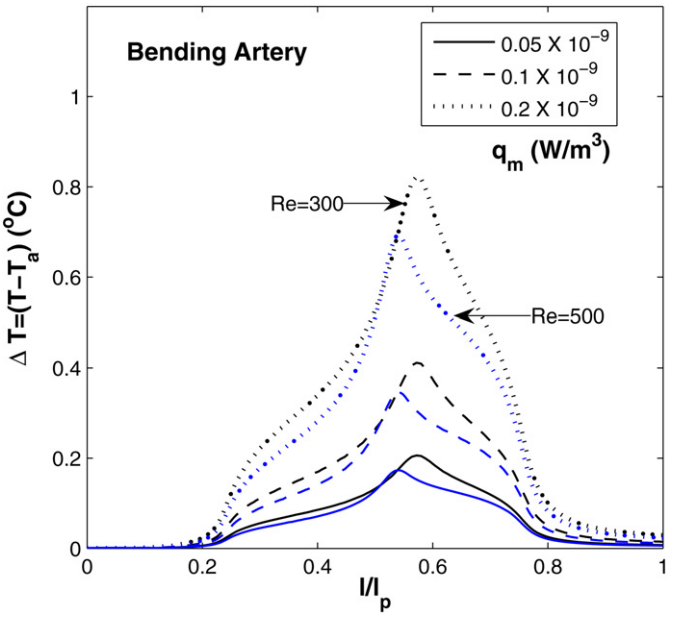

Fig. 4. Temperature change at the plaque/lumen interface produced by variations in the local heat generation in the plaque $\dot{q}_m$ for an arterial bend. In this figure, the macrophage layer dimensions are $l_{mp} = 1.500$ μm ($l_{mp} = l_p/2$) and $d_{mp} = 25$ μm, $d_p = 540$ μm, and $l_f = 50$ μm. The black lines correspond to $Re = 300$ and the gray lines represent $Re = 500$.

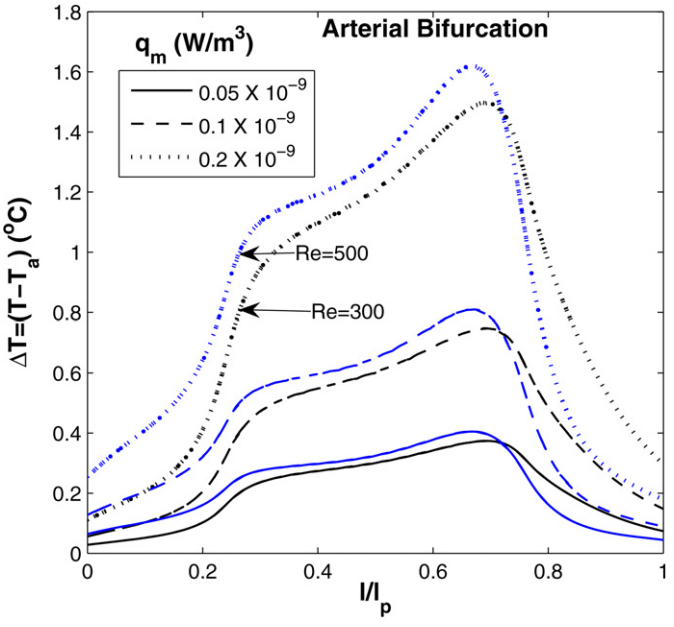

Fig. 5. Temperature change at the plaque/lumen interface produced by variations in the local heat generation in the plaque $\dot{q}_m$ for an arterial bifurcation. In this figure, the macrophage layer dimensions are $l_{mp} = 1.500$ μm ($l_{mp} = l_p/2$) and $d_{mp} = 25$ μm, $d_p = 670$ μm, and $l_f = 50$ μm. The black lines correspond to $Re = 300$ and the gray lines represent $Re = 500$.

the maximum temperature is registered at the downstream edge of the plaque. This difference is resulted from the presence of flow separation at the bending artery and the flow circulation observed at the arterial bifurcation, respectively. These flow instabilities depend on the arterial geometry, plaque size, and the magnitude of the blood velocity registered during the cardiac

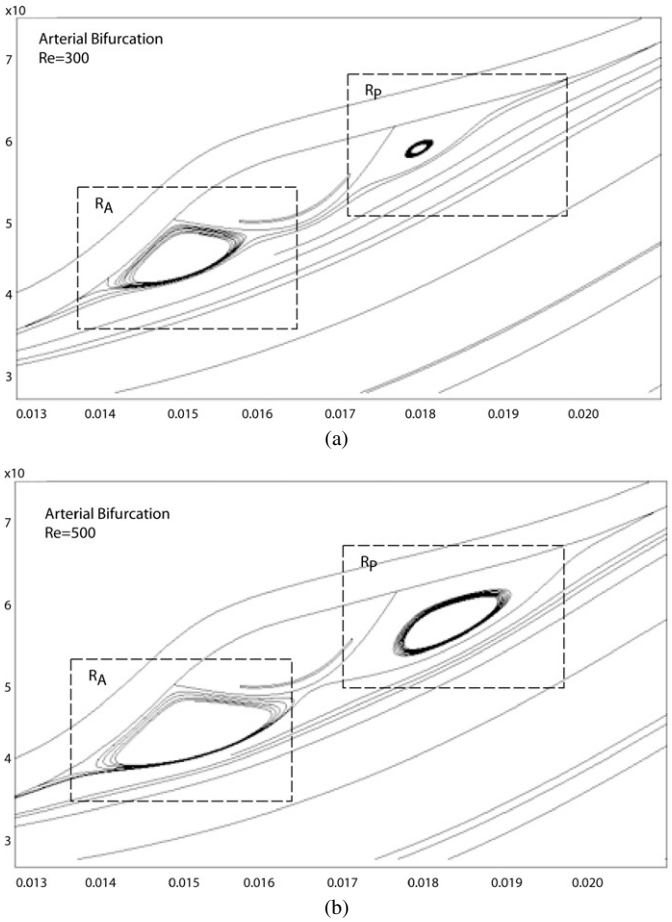

Fig. 6. Flow circulation observed around an inflamed plaque located in an arterial bifurcation. Results shown correspond to two different Reynolds numbers ($Re = 300$ and $Re = 500$) and $\dot{q}_m = 0.1$ W mm^{-3}, $d_p = 670$ μm, $d_{mp} = 25$ μm, $l_f = 100$ μm and $l_{mp} = 1500$ μm.

cycle. Figs. 6(a) and (b) show the flow circulation observed in an arterial bifurcation.

The blood flow in straight artery has no flow instabilities for the entire region of plaque, which forces ΔT_{max} to occur downstream near the end on the plaque. For the bending artery, the boundary layer is thinner at the upstream edge and encounters a separation point near the apex of the plaque. The thinner boundary layer contributes to the transport of thermal energy from the plaque surface to the blood flow, which explains the slow increase of ΔT observed at the upstream edge of the plaque (Fig. 4). In the bifurcation case of Fig. 5, blood flow of higher Reynolds number produces higher temperature distribution, which is contrary to the observations in the bending and straight arteries (Figs. 3 and 4). It is explained by the presence of circulation occurred in the regions surrounding the plaque as indicated in Figs. 6(a) and (b).

3.2. *Quantification of flow circulation*

To quantify the effect of flow circulation on the temperature in the plaque/lumen interface and the blood surrounding the plaque, the absolute circulation is calculated in the anterior and posterior regions of the plaque as indicated in Figs. 6(a) and (b).

Table 3
Average absolute circulation modified or absolute circulation (Γ_{ABS}/A_{tot}) in the anterior (R_A) and posterior (R_P) regions of an atherosclerotic plaque located in an arterial bifurcation

Re no.	R_A	R_P
300	87.1	101.5
400	105.2	120.2
500	122.9	139.5
600	140.0	159.2

The relationship for Γ_{ABS}/A_{tot} measured in s^{-1}, is obtained from [39], where Γ_{ABS} is the modified or absolute circulation parameter, and A_{tot} is the total wetted area over which Γ_{ABS} is calculated. The velocity profile is calculated considering the geometry indicated in Fig. 1 and following parameters: $\dot{q}_m = 0.1\ W\,mm^{-3}$, $d_p = 670\ \mu m$, $d_{mp} = 25\ \mu m$, $l_f = 100\ \mu m$ and $l_{mp} = 1500\ \mu m$.

These figures show the stream lines associated to the blood flow in the arterial lumen. The absolute circulation is calculated based on [39], using the equation $\Gamma_{ABS}/A_{tot} = (\Sigma|\xi|\Delta A)/A_{tot}$, where A_{tot} is the total wetted area of the region of interest, ξ is the vorticity calculated by the curl of the velocity field, and ΔA represents the area of each mesh element inside the interest region. The values of the absolute or modified circulation (Γ_{ABS}/A_{tot}) are calculated for the different Reynolds numbers considered, and are given in Table 3. These calculations are presented to quantify the flow structure near the plaque and relate such property to the temperature variation observed in the blood near the inflamed plaque. Figs. 7(a) and (b) show a series of temperature contours surrounding the plaque in an arterial bifurcation. As blood flow increases, heat transport is reduced due to flow circulation, which decreases cooling effect of blood flow.

3.3. Variation of d_{mp}

As another important factor affecting the temperature distribution, macrophage layer thickness d_{mp} is varied. It is observed that as the macrophage layer thickness d_{mp} increases, the maximum temperature ΔT_{max} increases proportionally in all the arterial cases studied. Figs. 8 and 9 show the cases of straight artery and arterial bifurcation. Particularly, the increase of d_{mp} of 100% produce an average ΔT_{max} increase of 92, 90 and 94% for the straight, bending and bifurcation cases, respectively. The linear relationship between the macrophage layer thickness d_{mp} and the maximum temperature change ΔT_{max} are shown in Fig. 10, which is also observed in experimental studies [3,38]. The slopes of the linear functions are presented in Table 4, depending on the arterial geometry as well as other plaque parameters.

3.4. Variation of l_f

The distance between the macrophage layer and the plaque/lumen interface is referred as fibrous cap thickness l_f. While the variation of ΔT by means of fibrous cap thickness (l_f) is relatively smaller than other factors as shown in Fig. 11, it is also an important parameter affecting the thermal stability of the atherosclerotic plaque. Fig. 12 shows how ΔT_{max} is reduced as the magnitude of l_f is increased in all the vessels studied. The

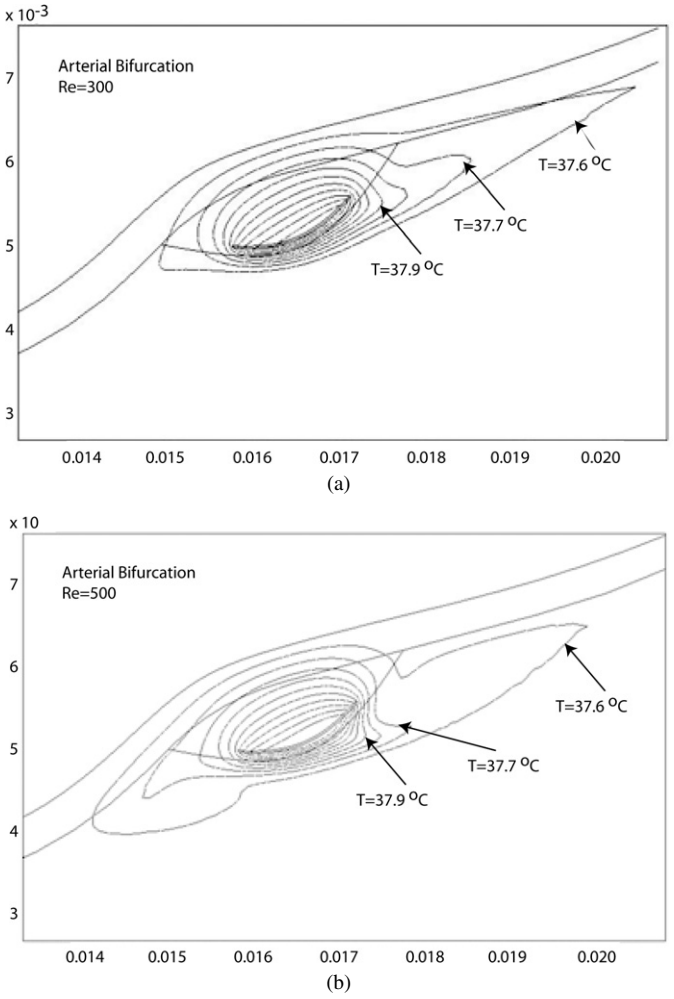

Fig. 7. Temperature contours around an inflamed plaque located in an arterial bifurcation. Results shown correspond to two different Reynolds numbers ($Re = 300$ and $Re = 500$) and $\dot{q}_m = 0.1\ W\,mm^{-3}$, $d_p = 670\ \mu m$, $d_{mp} = 25\ \mu m$, $l_f = 100\ \mu m$ and $l_{mp} = 1500\ \mu m$.

Table 4
Values of slope (m) and intercept (b) for Fig. 10 where the lines $\Delta T_{max} = b + m d_{mp}$ are shown.

Vessel type	m	b	r
Straight	0.0193	0.0819	0.9992
Bending	0.0148	0.0476	0.9999
Bifurcation	0.0278	0.0641	0.9999

These calculations correspond to the following parameters: $\dot{q}_m = 0.1\ W\,mm^{-3}$, $l_f = 50\ \mu m$, $Re = 300$, and $d_p = 500$ (straight), 540 (bending), 670 (bifurcation) μm.

inverse relationship between the maximum temperature and the fibrous cap thickness are presented in Table 5, and also observed in experimental study [3].

3.5. Variation of d_p

The effect of the plaque size is considered by varying the parameter d_p, that is, plaque thickness. The calculations performed for $d_p = 250$, 500 and 750 μm, indicate that the variations in the plaque size does not affect the temperature on the

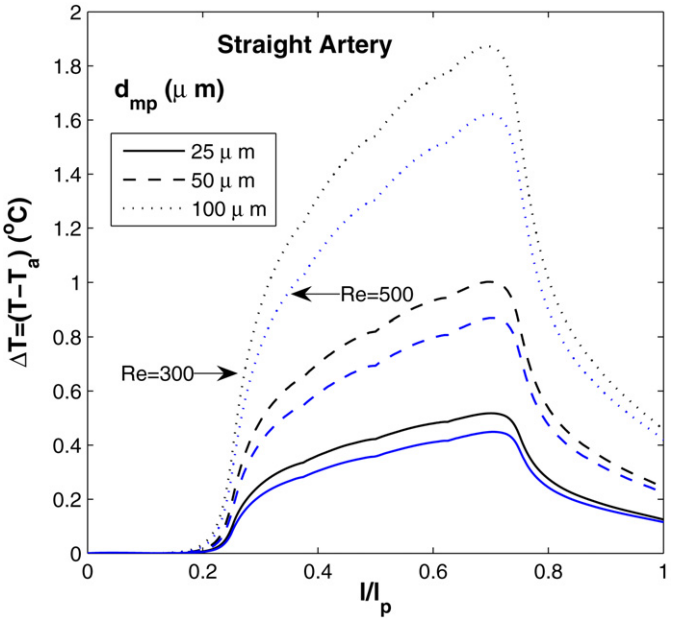

Fig. 8. Temperature change at the plaque/lumen interface produced by variations in the macrophage thickness d_{mp}. This results correspond to the straight artery with $\dot{q}_{\mathrm{m}} = 0.1\ \mathrm{W\,mm^{-3}}$, $l_{\mathrm{mp}} = 3335\ \mu\mathrm{m}$, $d_{\mathrm{p}} = 500\ \mu\mathrm{m}$, and $l_{\mathrm{f}} = 50\ \mu\mathrm{m}$. The black lines correspond to $Re = 300$ and the gray lines represent $Re = 500$.

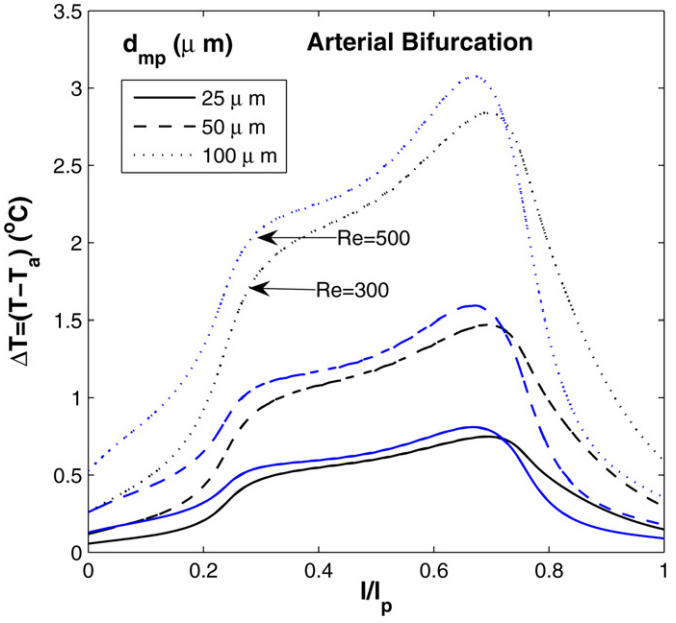

Fig. 9. Temperature change at the plaque/lumen interface produced by variations in the macrophage thickness d_{mp}. This results correspond to the arterial bifurcation with $\dot{q}_{\mathrm{m}} = 0.1\ \mathrm{W\,mm^{-3}}$, $l_{\mathrm{mp}} = 1.500\ \mu\mathrm{m}$, $d_{\mathrm{p}} = 670\ \mu\mathrm{m}$, and $l_{\mathrm{f}} = 50\ \mu\mathrm{m}$. The black lines correspond to $Re = 300$ and the blue lines represent $Re = 500$. (For interpretation of the references to color in this figure legend, the reader is referred to the web version of this article.)

plaque/lumen interface considerably for all the different arterial cases. With respect to variation of d_{p}, $\Delta T_{\max}$ varied between 6 and 10%. However, large increase of d_{p} implies that the vessel can be considerably occluded, which affects the characteristics of heat transfer as well as the blood flow at the region surrounding a plaque.

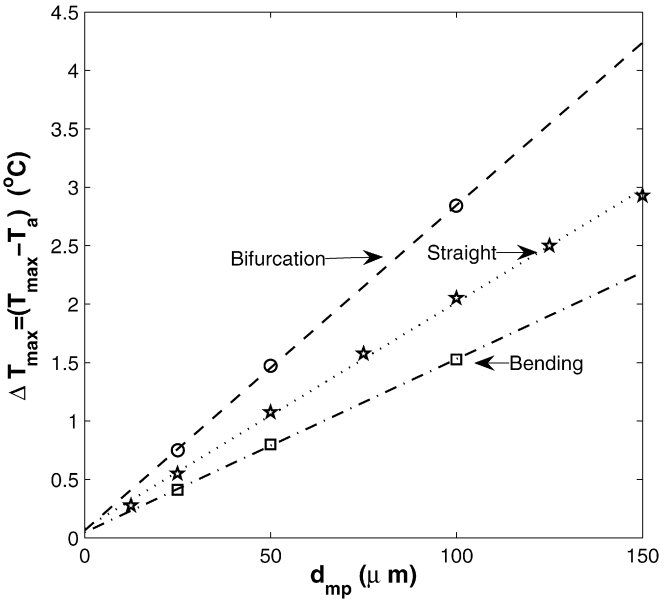

Fig. 10. Maximum temperature change $\Delta T_{\max}$ at the plaque/lumen interface produced by variations in the macrophage layer thickness d_{mp}. These results correspond to the three arterial geometries considered, and the calculations fit in the line $\Delta T_{\max} = b + m d_{\mathrm{mp}}$, where values for the constants b and m are given in Table 4 for each vessel geometry. These calculations correspond to $\dot{q}_{\mathrm{m}} = 0.1\ \mathrm{W\,mm^{-3}}$, $l_{\mathrm{f}} = 50\ \mu\mathrm{m}$, $Re = 300$, and $d_{\mathrm{p}} = 500$ (straight), 540 (bending), 670 (bifurcation) μm.

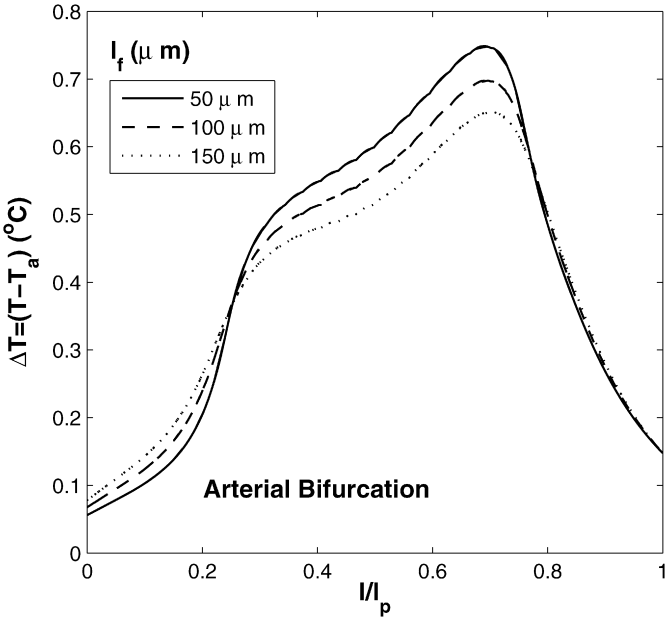

Fig. 11. Temperature change at the plaque/lumen interface produced by variations in the fibrous cap thickness l_{f} for an arterial bifurcation. Results shown correspond to $\dot{q}_{\mathrm{m}} = 0.1\ \mathrm{W\,mm^{-3}}$, $l_{\mathrm{mp}} = 1.500\ \mu\mathrm{m}$, $d_{\mathrm{p}} = 670\ \mu\mathrm{m}$, $d_{\mathrm{mp}} = 25\ \mu\mathrm{m}$ and $Re = 300$.

4. Conclusions

A numerical calculation of temperature distribution at plaque/lumen interface was carried out in three different arterial systems (straight artery, bending artery and arterial bifurcation). In these vessels, the plaques of different sizes with

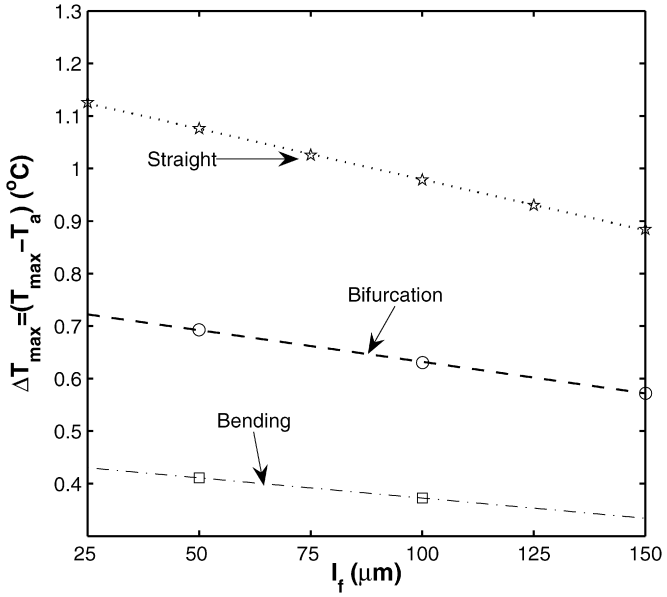

Fig. 12. Maximum temperature change $\Delta T_{\max}$ at the plaque/lumen interface produced by variations in the fibrous cap thickness l_{f} for the three arterial geometries. The data fits a straight line $\Delta T_{\max} = b + ml_{\mathrm{f}}$, where the values for the constants b and m are given in Table 5. Results shown correspond to $\dot{q}_m = 0.1\ \mathrm{W\,mm^{-3}}$, $d_{\mathrm{mp}} = 50\ \mu\mathrm{m}$, $Re = 300$, and $d_{\mathrm{p}} = 500$ (straight), 540 (bending), 670 (bifurcation) μm.

Table 5
Values of slope (m) and intercept (b) for Fig. 12 where the lines $\Delta T_{\max} = b + ml_{\mathrm{f}}$ are shown

Vessel type	m	b	r
Straight	−0.0019	1.1722	0.9999
Bending	−0.0008	0.4495	1.0000
Bifurcation	−0.0012	0.7521	0.9999

These calculations correspond to the following parameters: $\dot{q}_{\mathrm{m}} = 0.1\ \mathrm{W\,mm^{-3}}$, $d_{\mathrm{mp}} = 50\ \mu\mathrm{m}$, $Re = 300$ and $d_{\mathrm{p}} = 500$ (straight), 540 (bending), 670 (bifurcation) μm.

various inflammatory cells content and distributions were considered. The plaque was located at the region of low wall shear stress (WSS) as reported in the literature [12,14]. Due to the presence of the macrophage layer, a hot spot is registered at the plaque/lumen interface. Given the lack of measurements of the macrophage heat generation in atherosclerotic plaques, the magnitude of $\dot{q}_{\mathrm{m}}$ was assigned with the values of 0.05, 0.1 and $0.2\ \mathrm{W\,mm^{-3}}$.

It is shown that $\Delta T_{\max}$ is in general located behind the apex of the plaque; the location of $\Delta T_{\max}$ is governed by arterial geometry, flow instabilities such as flow separation and flow circulation, and distribution of macrophage layer. The occurrences of flow separation and circulation are observed in bending artery and arterial bifurcation, respectively. In bending artery, the thinner boundary layer before separation point enforces the convective cooling effect of blood flow at the upstream of the plaque. In arterial bifurcation, as blood velocity increases, the convective cooling effect is reduced with increasing the size of flow circulation over plaque/lumen surface.

From the parametric studies, metabolic heat generation q_{m} accounting for macrophage population and macrophage layer thickness d_{mp} have more influence over the plaque temperature. Meanwhile, plaque thickness d_{p} insignificantly affects the temperature on plaque/lumen interface. The variation of ΔT is in proportion to metabolic heat generation q_{m}, macrophage layer thickness d_{mp} and plaque thickness d_{p}, whereas varies inversely with fibrous cap thickness l_{f}.

ten Have et al. have reported that the temperature difference at the lumen depends on heat source size, source geometry and heat source production, but no arterial geometry effect was mentioned for temperature distribution because the geometry used for a model is only a straight tube of a coronary artery [10]. In our study, however, it is also observed that the effect of arterial geometry is one of the significant factors affecting temperature distribution and maximum temperature location because different geometries establish the different blood flow profiles and the occurrence of flow instabilities resulting in the variation of local heat transfer at the plaque/lumen interface. For example, compared the maximum temperature of straight artery case with other cases, those of the bending artery and the arterial bifurcation are approximately 20% lower and 60% higher, which show the flow instabilities.

Furthermore, arterial wall temperatures are significantly influenced by the blood flow running through the vessel which is referred as the cooling effect of blood flow [40]. Currently, the measurement using a catheter is subjected to large errors due to the cooling effect of blood flow [41,42]. In the presence of blood flow, the best spot to measure plaque temperature is between the middle and the far edge of the plaque where the point of maximum temperature can be located. It can be also postulated that direct measurements should be taken very close to the plaque/lumen surface. In our further studies, the transient cases with different physiological pulsatile flow conditions will be carried out to calculate the flow and temperature distributions. The inlet conditions of a waveform function will be modified for the flow condition such as normal cardiac cycles or occlusion cardiac cycles.

References

[1] M.J. Davies, A macro and micro view of coronary vascular insult in ischemic heart disease, Circulation 82 (3 suppl) (1990) II38–II46.
[2] D.E. Gutstein, V. Fuster, Pathphysiology and clinical significance of atherosclerotic plaque rupture, Cardiovascular Research 41 (1999) 323–333.
[3] M. Madjid, M. Naghavi, B.A. Malik, S. Litovsky, J.T. Wilerson, W. Casscells, Thermal detection of vulnerable plaque, American Journal of Cardiology 90 (2002) 36L–39L.
[4] A.M. Malek, S.L. Alper, S. Izumo, Hemodynamic shear stress and its role in atherosclerosis, Journal of the American Medical Association 282 (1999) 2035–2042.
[5] E. Falk, P.K. Shah, V. Fuster, Coronary plaque disruption, Circulation 92 (1995) 657–671.
[6] V. Fuster, Z.A. Fayad, J.J. Badimon, Acute coronary syndromes: Biology, Lancet 353 (Suppl 2) (1999) SII5–SII9.
[7] R. Corti, V. Fuster, J.J. Badimon, Pathogenetic concepts of acute coronary syndromes, Journal of the American College of Cardiology 41 (2003) 7S–14S.
[8] L. Diamantopoulos, Arterial wall thermography, Journal of Interventional Cardiology 16 (2003) 261–266.
[9] M. Naghavi, M. Madjid, K. Gul, S. Siadaty, S. Litovsky, J.T. Willerson, S.W. Casscells, Thermography basket catheter: In vivo measurement

of the temperature of atherosclerotic plaques for detection of vulnerable plaques, Catheterization in Cardiovascular Interventions 59 (2003) 52–59.
[10] A.G. ten Have, F.J.H. Gijsen, J.J. Wentzel, C.J. Slager, A.F.W. van der Steen, Temperature distribution in atherosclerotic coronary arteries: influence of plaque geometry and flow (a numerical study), Physics in Medicine and Biology 49 (2004) 4447–4462.
[11] C.W. Kerber, S.T. Hecht, K. Knox, R.B. Buxton, H.S. Meltzer, Flow dynamics in a fatal aneurism of the basilar artery, American Journal of Neuroradiology 17 (1996) 1417–1421.
[12] C.K. Zarins, D.P. Giddens, B.K. Bharadvaj, V.S. Sottiurai, R.F. Mabon, S. Glagov, Carotid bifurcation atherosclerosis: quantitative correlation of plaque localization with flow velocity profiles and wall shear stress, Circulation Research 53 (1983) 502–514.
[13] B.K. Bharadvaj, R.F. Mabon, D.P. Giddens, Steady flow in a model of the human carotid bifurcation, Part I – flow visualization, Journal of Biomechanics 15 (1982) 349–362.
[14] A. Gnasso, C. Irace, C. Carallo, M.S. De Franceschi, C. Motti, P.L. Mattioli, A. Pujia, In vivo association between low wall shear stress and plaque in subjects with asymmetrical carotid atherosclerosis, Stroke 28 (1997) 993–998.
[15] M. Motomiya, T. Karino, Flow patterns in the human carotid artery bifurcation, Stroke 15 (1984) 50–56.
[16] S. Wada, T. Karino, Theoretical prediction of low-density lipoproteins concentration at the luminal surface of an artery with a multiple bend, Annals of Biomedical Engineering 30 (2002) 778–791.
[17] R. Virmani, F.D. Kolodgie, A.P. Burke, A. Farb, S.M. Schwartz, Lessons from sudden coronary death: A comprehensive morphological classification scheme for atherosclerotic lesions, Arteriosclerosis Thrombosis, and Vascular Biology 20 (2000) 1262–1275.
[18] D.K. Stangeby, C.R. Ethier, Computational analysis of coupled blood-wall arterial LDL transport, Journal of Biomechanical Engineering 124 (2002) 1–8.
[19] T. Asakura, T. Karino, Flow patterns and spatial distribution of atherosclerotic lesions in human coronary arteries, Circulation Research 66 (1990) 1045–1066.
[20] K. Perktold, M. Resch, R.O. Peter, Three-dimensional numerical analysis of pulsatile flow and wall shear stress in the carotid artery bifurcation, Journal of Biomechanics 24 (1991) 409–420.
[21] N. Filipovic, M. Kojic, Computer simulations of blood flow with mass transport through the carotid artery bifurcation, Theoretical and Applied Mechanics 31 (2004) 1–33.
[22] G. Rappitsch, K. Perktold, Computer simulation of convective diffusion processes in large arteries, Journal of Biomechanics 29 (1996) 207–215.
[23] G. Rappitsch, K. Perktold, Pulsatile albumin transport in large arteries: a numerical simulation study, Journal of Biomechanical Engineering 118 (1996) 511–519.
[24] C.G. Caro, T.J. Pedley, R.C. Schroter, W.A. Seed, The Mechanics of the Circulation, Oxford Medical, New York, 1978.
[25] X. He, D.N. Ku, Unsteady entrance flow development in a straight tube, Journal of Biomechanical Engineering 116 (1994) 355–360.
[26] W. Jessup, A. Baoutina, L. Kritharides, The Macrophage: Macrophages in Cardiovascular Disease, Oxford Univ. Press, Oxford, UK, 2002, pp. 490–522.
[27] S. Verheye, G.R.Y. De Meyer, G. Van Langenhove, M.W.M. Knaapen, M.M. Kockx, In vivo temperature heterogeneity of atherosclerotic plaques is determined by plaque composition, Circulation 105 (2002) 1596–1601.
[28] Y.C. Fung, Biomechanics: Circulation, second ed., Springer-Verlag, New York, 1996.
[29] S.Z. Zhao, X.Y. Xu, A.D. Hughes, S.A. Thom, A.V. Stanton, B. Ariff, Q. Long, Blood flow and vessel mechanics in a physiologically realistic model of a human carotid arterial bifurcation, Journal of Biomechanics 33 (2000) 975–984.
[30] V. Bhatia, R. Bhatia, S. Dhindsa, M. Dhindsa, Imaging of the vulnerable plaque: New modalities, Southern Medical Journal 96 (2003) 1142–1147.
[31] G. Rappitsch, K. Perktold, E. Pernkopf, Numerical modeling of shear-dependent mass transfer in large arteries, International Journal for Numerical Methods in Fluids 25 (1997) 847–857.
[32] B.M. Johnston, P.R. Johnston, S. Corney, D. Kilpatrick, Non-Newtonian blood flow in human right coronary arteries: Transient simulations, Journal of Biomechanics 39 (2006) 1116–1128.
[33] J. Bale-Glickman, K. Selby, D. Saloner, O. Savas, Experimental flow studies in exact-replica phantoms of atherosclerotic carotid bifurcations under steady input conditions, Journal of Biomechanical Engineering 125 (2003) 38–48.
[34] J.W. Valvano, B. Chitsabesan, Thermal conductivity and diffusivity of arterial wall and atherosclerotic plaque, Lasers in the Life Sciences 1 (1987) 219–229.
[35] F.A. Duck, Physical Properties of Tissue: A Comprehensive Reference Book, Academic Press, San Diego, CA, 1990.
[36] A.J. Welch, M.J.C. Van Gemert, Optical Thermal Response of Laser-Irradiated Tissue, Plenum, New York, 1995.
[37] S.A. Thoren, M. Monti, B. Holma, Heat conduction microcalorimetry of overall metabolism in rabbit alveolar macrophages in monolayers and in suspensions, Biochimica et Biophysica Acta 1033 (1990) 305–310.
[38] W. Casscells, X. Hathorn, M. David, T. Brabach, W.K. Vaughn, H.A. McAllister, G. Bearman, J.T. Willerson, Thermal detection of cellular infiltrates in living atherosclerotic plaques: Possible implications for plaque rupture and thrombosis, Lancet 347 (1996) 1447–1449.
[39] D.W. Crowder, P. Diplas, Vorticity and circulation: spatial metrics for evaluating flow complexity in stream habitats, Canadian Journal of Fisheries and Aquatic Sciences 59 (2002) 633–645.
[40] C. Stefanadis, K. Toutouzas, M. Vavuranakis, E. Tsiamis, S. Vaina, P. Toutouzas, New balloon-thermography catheter for in vivo temperature measurements in human coronary atherosclerotic plaques: A novel approach for thermography? Catheterization and Cardiovascular Interventions 58 (2003) 344–350.
[41] L. Diamantopoulos, X. Liu, I.D. Scheerder, R. Krams, S. Li, J.V. Cleemput, W. Desmet, P.W. Serruys, The effect of reduced blood-flow on the coronary wall temperature: Are significant lesions suitable for intravascular thermography? European Heart Journal 24 (2003) 1788–1795.
[42] C. Stefanadis, K. Toutouzas, E. Tsiamis, I. Mitropoulos, C. Tsioufis, I. Kallikazaros, C. Pitsavos, P. Toutouzas, Thermal heterogeneity in stable human coronary atherosclerotic plaques is underestimated in vivo: the cooling effect of blood flow, Journal of the American College of Cardiology 41 (2003) 403–408.